Nanoluciferase Reporter Mycobacteriophage for Sensitive and Rapid Detection of *Mycobacterium tuberculosis* Drug Susceptibility

Paras Jain,[a,b,c] Spencer Garing,[a]* Deepshikha Verma,[d] Rajagopalan Saranathan,[b] Nicholas Clute-Reinig,[a]* Jacob Gadwa,[d]* Chelsea Peterson,[d] Gleda Hermansky,[a] Anna Astashkina Fernandez,[a] Emmanuel Asare,[b,e] Torin R. Weisbrod,[b] Ethan Spencer,[a] Claire V. Mulholland,[b] Michael Berney,[b] David Bell,[f]* Kevin P. Nichols,[a]* Anne-Laure M. Le Ny,[a]* Diane Ordway,[d] ⬤ William R. Jacobs, Jr.,[b,g] Akos Somoskovi,[f]* ⬤ Kyle J. Minch[a]*

[a]Intellectual Ventures Laboratory, Bellevue, Washington, USA

[b]Department of Microbiology and Immunology, Albert Einstein College of Medicine, Bronx, New York, USA

[c]Trudeau Institute, Saranac Lake, New York, USA

[d]Mycobacteria Research Laboratories, Department of Microbiology, Immunology and Pathology, Colorado State University, Fort Collins, Colorado, USA

[e]Department of Pathology, Albert Einstein College of Medicine and Montefiore Medical Center, Bronx, New York, USA

[f]Intellectual Ventures' Global Good Fund, Bellevue, Washington, USA

[g]Department of Molecular Genetics, Albert Einstein College of Medicine, Bronx, New York, USA

ABSTRACT Phenotypic testing for drug susceptibility of *Mycobacterium tuberculosis* is critical to basic research and managing the evolving problem of antimicrobial resistance in tuberculosis management, but it remains a specialized technique to which access is severely limited. Here, we report on the development and validation of an improved phage-mediated detection system for *M. tuberculosis*. We incorporated a nanoluciferase (Nluc) reporter gene cassette into the TM4 mycobacteriophage genome to create phage TM4-nluc. We assessed the performance of this reporter phage in the context of cellular limit of detection and drug susceptibility testing using multiple biosafety level 2 drug-sensitive and -resistant auxotrophs as well as virulent *M. tuberculosis* strains. For both limit of detection and drug susceptibility testing, we developed a standardized method consisting of a 96-hour cell preculture followed by a 72-hour experimental window for *M. tuberculosis* detection with or without antibiotic exposure. The cellular limit of detection of *M. tuberculosis* in a 96-well plate batch culture was $\leq 10^2$ CFU. Consistent with other phenotypic methods for drug susceptibility testing, we found TM4-nluc to be compatible with antibiotics representing multiple classes and mechanisms of action, including inhibition of core central dogma functions, cell wall homeostasis, metabolic inhibitors, compounds currently in clinical trials (SQ109 and Q203), and susceptibility testing for bedaquiline, pretomanid, and linezolid (components of the BPaL regimen for the treatment of multi- and extensively drug-resistant tuberculosis). Using the same method, we accurately identified rifampin-resistant and multidrug-resistant *M. tuberculosis* strains.

IMPORTANCE *Mycobacterium tuberculosis*, the causative agent of tuberculosis disease, remains a public health crisis on a global scale, and development of new interventions and identification of drug resistance are pillars in the World Health Organization End TB Strategy. Leveraging the tractability of the TM4 mycobacteriophage and the sensitivity of the nanoluciferase reporter enzyme, the present work describes an evolution of phage-mediated detection and drug susceptibility testing of *M. tuberculosis*, adding a valuable tool in drug discovery and basic biology research. With additional validation, this system may play a role as a quantitative phenotypic reference method and complement to genotypic methods for diagnosis and antibiotic susceptibility testing.

Tuberculosis (TB), caused by *Mycobacterium tuberculosis*, is a disease with an effective
antibiotic therapy consisting of a combination of 4 antibiotics taken for 6 months;
however, the emergence of strains with fewer options for curative therapy (multi-,
extensively, and totally drug-resistant strains [MDR-TB, XDR-TB, and TDR-TB, respec-
tively]) presents a public health threat and underscores the need for advancements in
tools to facilitate new drug development as well as to diagnose and effectively treat this
disease (1, 2). Accordingly, intensified research on interventions and identification of
drug resistance to guide appropriate therapy are pillars in the WHO End TB Strategy for
disease elimination (1, 3).

For drug susceptibility testing (DST), methods are broadly divided between pheno-
typic and genotypic approaches. Genotypic assays are attractive due to their rapid
turnaround time and capacity to probe multiple predetermined loci in a single reaction
(4–6). While data considering diverse antibiotics and multiple resistance loci in *M.
tuberculosis* are accumulating from next-generation sequencing efforts (7), genotypic
DST is most effective for drugs with well-defined resistance mutations, as in the
GeneXpert *M. tuberculosis*/RIF Ultra test (8). Identification of MDR-TB and XDR-TB is
more complex, in part due to our incomplete understanding of resistance mutations to
all the 10-plus antibiotics that can be used in these treatment regimens and the
potential for new mutations to arise (9). Recent results with a streamlined MDR/XDR
treatment regimen (bedaquiline, pretomanid, and linezolid [BPaL]) demonstrate the
efficacy of simplified therapy for drug-resistant tuberculosis (10, 11); however, resis-
tance mutations are still being identified, and phenotypic testing is necessary for initial
identification of these (12). Thus, the diversity of antibiotics used to treat TB, and the
lack of correlation between a genotype and the resulting phenotypic resistance, call for
complementary approaches in both viability monitoring to identify genotype-to-
phenotype correlations in basic research, as well as for clinical reference.

For decades, phenotypic growth-based assays have been a reference method for *M.
tuberculosis* detection and quantitative DST and are critical for identifying resistance
mutations that can be probed in rapid genotypic tests (13). These approaches are
appealing in that they provide a readout of viability and/or drug susceptibility based on
detection of expanding bacterial populations and are generally agnostic to antibiotic
mechanism or prospective knowledge of underlying resistance mutations. For drug-
susceptible cells responding to antibiotic treatments, metabolic homeostasis is com-
promised, whereas the drug-resistant cells exposed to antibiotic treatment maintain
homeostasis and division. The potency of a given compound against *M. tuberculosis* is
subsequently quantified by measuring whole-cell responses across a range of treat-
ment concentrations, which correspondingly allows for interpretation of the level of
resistance or susceptibility that an *M. tuberculosis* strain exhibits against an antibiotic.

Two common measures of antibiotic potency/*M. tuberculosis* susceptibility are
minimal bactericidal concentration (MBC) and the MIC. MBC assays define the ability of
a test compound to kill *M. tuberculosis*, whereas MIC values describe the concentration
at which an antibiotic inhibits growth to a defined level (typically reported at 95 or
99%) compared to untreated control cells (14, 15). While the MBC and MIC are both
variations on the theme of DST and broad "viability monitoring" because the MBC
requires distinct exposure and recovery/regrowth periods, they are a preferred research
tool for identification and characterization of anti-TB agents (15). MIC data have been
widely used by WHO to define the critical concentrations, epidemiological cutoff values
(ECOFFs), and clinical breakpoint of anti-TB agents to guide individual clinical decisions
in patient treatment (16).

Multiple approaches, including the agar proportion method, Mycobacterial Growth
Indicator Tube (MGIT) system (17), microscopic observation of drug susceptibility
(MODS) (18), and Sensititre broth microdilution assays (19), can be used to determine

MIC and MBC values; however, the time to result is dependent on the starting inoculum, and, in the case of *M. tuberculosis* with a doubling time of >16 hours, a positive culture result requires days to weeks of incubation. Recognizing the need for accurate drug susceptibility testing and as a complement to the increasing potential of decentralized DST by genotypic methods, different strategies have been developed to decrease the time to result of replication-based phenotypic assays (20, 21). In addition to these, phenotypic methods that rely on increasingly sensitive detection of proxy (nonreplication) signals while still maintaining the genotype-agnostic features of a growth-based viability detection assay are a parallel path for understanding the response of *M. tuberculosis* to a test condition (22).

Reporter mycobacteriophage systems represent a method for deriving phenotypic data in a replication-independent system, maintaining high sensitivity while reducing the time to result attendant with growth-based methods (23). Mycobacteriophages are viruses specific to mycobacteria and require viable *M. tuberculosis* for their propagation. In reporter systems, the virus attaches to cell surface and injects its genetic material into the susceptible host, which then transcribes and translates the foreign DNA, including the reporter gene (24). Inhibition of *M. tuberculosis* homeostasis by various antibiotics inhibits the expression of the reporter gene and compromises signal, thus providing a readout analogous to other growth/culture-based phenotypic assays but in a faster time frame. The first reporter mycobacteriophage was derived from mycobacterio-phage TM4 engineered to encode a firefly luciferase (ffLuc) gene cassette (25). The performance of this system was subsequently improved through methods development (26) and phage modifications (27, 28), enabling studies using phage for *M. tuberculosis* detection and DST from isolates and clinical specimens (29, 30). Additional phage modifications, including the introduction of a stronger constitutive promoter and use of reporter cassettes encoding one or more fluorescent proteins (fluo-rophages), enabled differentiation of antibiotic tolerance versus resistance in a mixed bacterial population, measurement of bactericidal activity of antibiotics against *M. tuberculosis in vitro* and in *ex vivo* sputum samples from TB patients, and DST assays directly on sputum samples from TB patients identifying rifampin heteroresistance (31–35). The combined conclusions of these efforts indicate that it is possible to use the TM4 mycobacteriophage encoding different reporter gene cassettes for DST and to measure bactericidal activity of anti-*M. tuberculosis* agents. The existing reporter phages, however, require sophisticated infrastructure to measure signal (fluorescence microscopy or flow cytometry), or, in the case of luciferase reporters to date, maximum sensitivity or signal stability is compromised due to intrinsic properties of the luciferase implemented (31, 32, 34, 36).

In an effort to improve the performance of previously described TM4 systems, in the present work, we created a TM4 phage vector that delivers a gene cassette of the nanoluciferase (Nluc) reporter enzyme (36; https://www.promega.com/resources/technologies/nanoluc-luciferase-enzyme/), which we term "TM4-nluc." We tested this TM4-nluc phage on auxotrophic and virulent clinical *M. tuberculosis* strains, assessing cellular limit of detection and compatibility with antibiotic susceptibility testing from a range of antibiotic classes/mechanisms of action. We found that following a preculture period, using TM4-nluc, the cellular limit of detection was on the order of high tens/low hundreds of *M. tuberculosis* cells and that in a 72-hour combined drug treatment/phage infection, we could identify drug susceptibility consistent with WHO-endorsed treatment concentrations to first-line antibiotics (rifampin, isoniazid, and ethambutol), a suite of second-line antibiotics, including all components of the BPaL regimen (be-daquiline, pretomanid, and linezolid), as well as compounds currently in trials to assess efficacy as TB therapeutics (SQ109 and Q203). In summary, we report here on the development, and methods to use, of an improved detection assay that is capable of identifying very low numbers of *M. tuberculosis* cells in batch culture, as well as drug susceptibility testing for antibiotics with mechanisms of action ranging from core "central dogma" functions (transcription, translation, and DNA replication) to metabolic and cell wall homeostasis, all in a 72-hour drug exposure-to-result time period.

RESULTS

Generation of TM4-nluc phage and methods for its use. Similar to firefly luciferase (ffLuc), Nluc allows for detection of batch signal from cells in well plate format; however, compared to ffLuc, Nluc generates a >10-fold-brighter signal on a molecule-per-molecule basis and utilizes a furimazine substrate that does not require ATP for light generation (37). Based on these reported performance characteristics of Nluc, we modified the parent phAE159 mycobacteriophage genome by cloning an *M. tuberculosis* codon-optimized Nluc gene ($nluc_{mtb}$) (see Fig. S1 in the supplemental material) downstream of the constitutively active L5 promoter ($PL_{L5}:nluc_{mtb}$) (31, 38). We term this new phage reagent "TM4-nluc."

Following generation of the base TM4 reporter construct, we proceeded with propagation of the phage stock as described previously (see Materials and Methods and reference 31). The *Mycobacterium smegmatis* plate harvest method yielded crude phage stocks in MP buffer in the range of 109 to 1,010 PFU/ml; however, due to the constitutively active nature of the promoter controlling reporter gene expression and the stability of Nluc, we observed high levels of active/functional Nluc as a by-product in phage preps, which, if left intact, diminished signal/noise ratios and compromised sensitivity in downstream experiments and assays. We assessed multiple methods for purifying contaminating Nluc away from TM4-nluc phage and ultimately identified two protocols (see Materials and Methods) that provided an optimal balance between phage purity and viability. Whether performing purification by ultracentrifugation or a multistep protocol incorporating centrifugation, anion-exchange chromatography, and hydrophobic interaction chromatography in the purified TM4-nluc phage preps, the background Nluc activity was reduced by >3 log. When normalized to PFU, there was <1-log phage loss between the initial and purified TM4-nluc phage preps.

With purified TM4-nluc in hand, we developed an experimental system to assess this new reporter reagent for viability of *M. tuberculosis* in the context of (i) sensitivity/cellular limit of detection and (ii) drug susceptibility/resistance testing. The workflow is presented schematically in Fig. 1 and Fig. S2 and described in greater detail in the subsequent text.

During the course of development, we identified critical components for maximizing assay performance. We observed that a "preculture" period maximizes signal/noise ratios of the viability assay. Accordingly, in our *in vitro* system, *M. tuberculosis* cells (virulent or auxotroph) were inoculated to a low target cell density and incubated at 37°C for 72 hours (~3 to 4 doublings for *M. tuberculosis* strains reported here). Although the exact mechanism is unclear, the presence of detergents commonly used in *M. tuberculosis* culture strongly inhibits phage infection and removal of detergent, and subsequent incubation in detergent-free medium was critical in maximizing signal/noise. Following equilibration in detergent-free medium, the *M. tuberculosis* cells were used in detection/viability monitoring assays in 96-well plate format (with or without antibiotic exposure). Independent of the treatment parameters of an experiment, in this system, TM4-nluc phage was added at a multiplicity of infection (MOI) >1 and <1,000 and incubated for 24 hours at 37°C. At the conclusion of the 24-hour infection/incubation, a fixed amount of Nluc substrate, Nano-Glo, was added to the wells, and a luminescent signal was measured by standard plate reader.

Whether conducting experiments for strict *M. tuberculosis* detection or DST, this TM4 system is a reporter of metabolic activity in the cells. In the event that viable cells with intact metabolic homeostasis are present, the TM4-nluc phage infect *M. tuberculosis*, and the $PL_{L5}:nluc_{mtb}$ expression cassette is transcribed and translated, resulting in reporter enzyme production. Due to the temperature-sensitive nature of the phage, this incubation at 37°C should not lead to lysis of *M. tuberculosis* cells, and the majority of enzyme remains intracellular; however, in experiments that implemented filter plates and vacuum washing of infected cells to reduce further background Nluc, we observed a reduction in overall signal from washed assay compared to the no-wash assay format (Fig. S3). This result suggests that enzyme exists in the extracellular milieu due to either
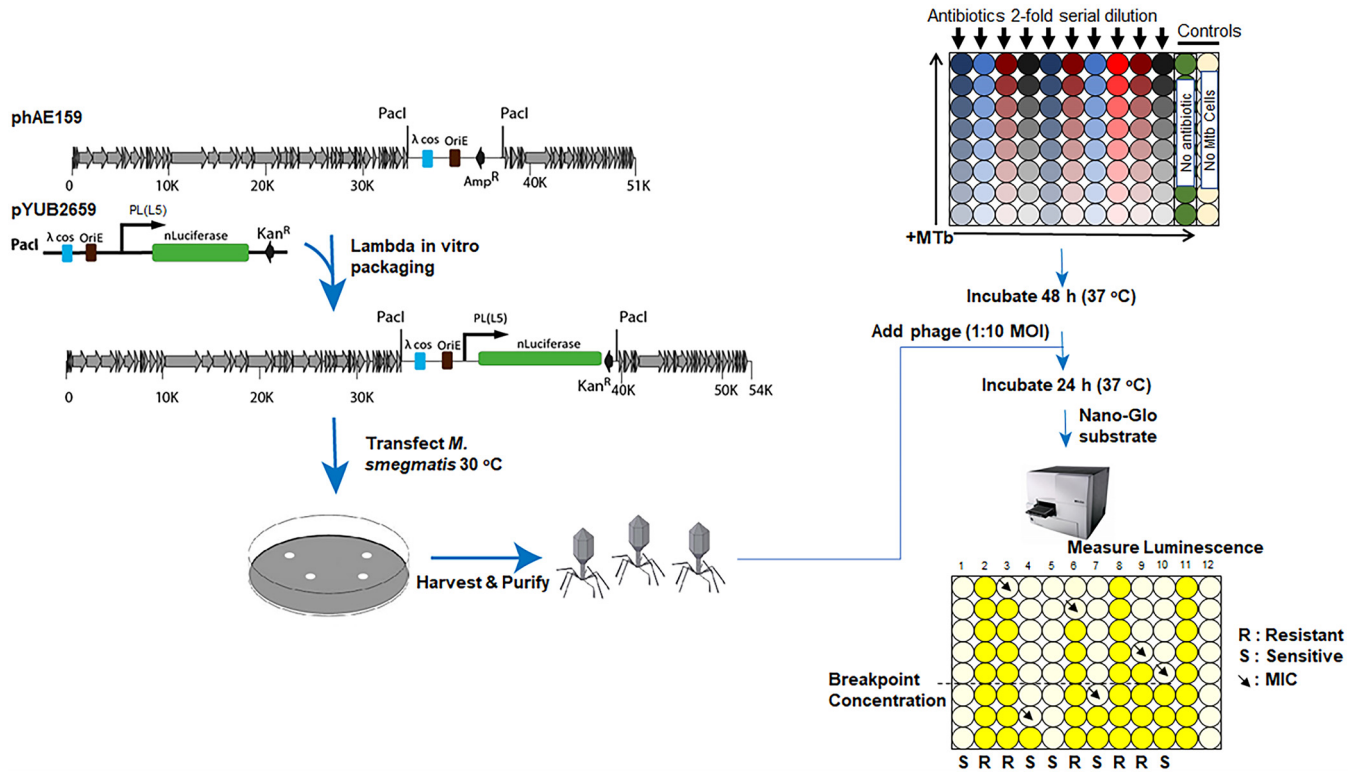
FIG 1 Schematic overview of phage reporter construct and method. TM4-nluc derives from modifying the pYUB2659 vector with a nanoluciferase gene cassette codon optimized for expression in *M. tuberculosis* (MTb). Following methods in reference 60, the reporter gene cassette was inserted into the phAE159 (TM4) backbone. Following lambda phage *in vitro* packaging, the reporter phasmid was transfected into *M. smegmatis* for phage amplification and expansion. TM4-nluc was sequentially purified (see Materials and Methods) prior to being deployed in *M. tuberculosis* detection or DST assays. Shown here, DST assays were conducted on uniform *M. tuberculosis* CFU inputs in each well with a 2-fold serial dilution of antibiotics (95 μl) proceeding down columns of a 96-well microtiter plate. After a 48-hour incubation period at 37°C in which *M. tuberculosis* cells were exposed to antibiotics (or control conditions), 5 μl phage was added to the appropriate wells, and the plate was returned to 37°C for a 24-hour infection/incubation. Following the 24-hour infection, 50 μl Nano-Glo substrate (prepared to manufacturer instructions) was added, and plates were read immediately on a BioTek Synergy H1 plate reader (refer to Materials and Methods). In the schematic depicted here, column 1 is populated by complete drug-sensitive *M. tuberculosis* cells (S); the drug treatment inhibits nanoluciferase production corresponding to a decrease in light signal generation. Column 2 is populated by complete drug-resistant cells (R), with maximum nanoluciferase production and light generation independent of the antibiotic concentration. Reading from top to bottom, black arrows indicate the drug dilution where antibiotic exposure falls below an inhibitory threshold above which nanoluciferase light production is inhibited and below which nanoluciferase light production approaches the untreated controls. Control wells include cells only, no phage; cells plus phage, no antibiotic; phage only, no cells; and empty medium wells.

protein translocation or cell lysis and underscores the importance of phage production/purification to optimize signal/noise in a one-pot assay.

Phage-mediated *M. tuberculosis* limit of detection is ≤10² CFU, and signal improves with increased culture acclimation time. Using the general method described above as a template, we assessed the cellular limit of detection (LOD) using TM4-nluc. In these experiments, cells were precultured as described above and in Materials and Methods and diluted in 10-fold serial steps. For these experiments, we investigated if an extended acclimation period in the plate (after transfer to detergent-free medium) affected the apparent relative luminescent unit (RLU) signal cellular LOD of the system. Accordingly, cells were inoculated in the plate and either immediately infected with TM4-nluc and incubated overnight at 37°C (Fig. 2A) or inoculated into the 96-well plate and allowed to equilibrate in the plate with detergent-free media for 48 hours prior to infection with TM4-nluc and overnight incubation (Fig. 2B). Immediately prior to phage addition, an aliquot of cells was removed, diluted in media containing detergent, and plated on 7H10 plates for CFU enumeration. From these data, we calculated the cellular LOD using the method described in reference 39 implemented in R using package drc (40) for nonlinear regression. We fitted the dose-response curve with a 4-parameter logistic function (with 1/signal weighting) and determined the LOD as the concentration at which the lower bound of the 95% signal
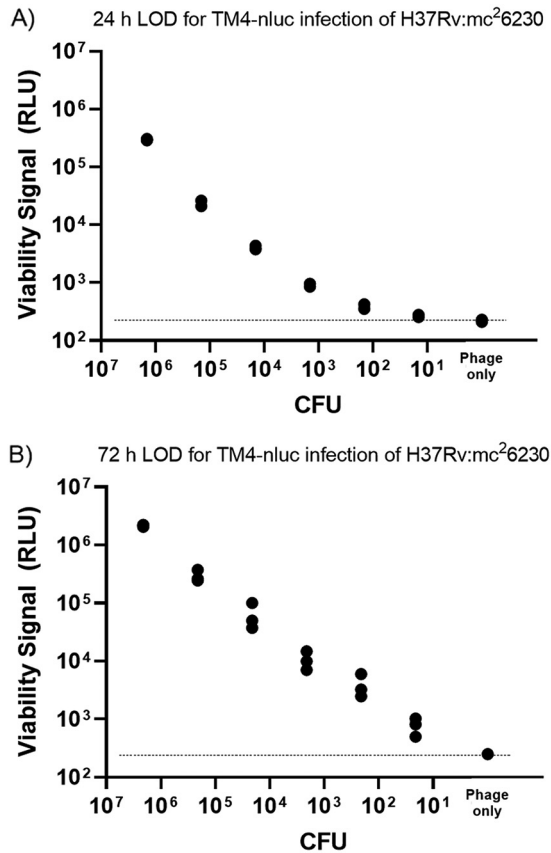
A)   24 h LOD for TM4-nluc infection of H37Rv:mc²6230

B)   72 h LOD for TM4-nluc infection of H37Rv:mc²6230

FIG 2 Phage-mediated *M. tuberculosis* limit of detection is ≤10² CFU, and signal improves with increased culture acclimation time. After a preculture period in rich growth medium with detergent, *M. tuberculosis* cells were washed and resuspended in rich growth medium without detergent and inoculated in 10-fold serial dilution into 96-well microtiter plates. Phage was added immediately after transition to detergent-free medium to determine the 24-h LOD (A) or given a 48-hour acclimation period in the detergent-free growth medium followed by phage addition and 24 h of incubation to determine the 72-h LOD (B). Dashed lines indicate the noise floor as determined by phage-only background RLU (average of RLU from phage-only wells; *n* = 3). In both cases, the cellular limit of detection is in the range of low 10² CFU/well.

confidence interval equals the upper bound of the 95% signal confidence interval of the blank. The signal standard error of the positive samples was estimated as the pooled standard error of the lowest 3 positive samples. With this method, we determined the bounds of our limit of detection to be in the low hundreds of *M. tuberculosis* CFU. The overall RLU signals across the cell concentration range were higher for the 72-hour total assay time condition, and we note that, despite an additional 48 hours in plate at 37°C, the cell numbers per well are not dramatically different between the 24- and 72-hour conditions, corresponding to less than 1 cell division for cells in well, indicating the importance of metabolic adaptation to enhance signal output after TM4-nluc phage infection (see Discussion).

Seventy-two-hour drug susceptibility testing of auxotroph and virulent *M. tuberculosis* strains with a panel of diverse antibiotics. With TM4-nluc and this experimental system to interrogate *M. tuberculosis* cell health, we next looked at this system for viability testing in the context of antibiotic treatment. As an extension of the LOD results described above, in order to maximize signal/noise over our phage-only background for these experiments, we targeted an inoculation of high 10⁵ to 10⁶ *M. tuberculosis* CFU/well in a 96-well plate. We followed a protocol most closely resembling the 72-hour assay from above and used the pansusceptible *M. tuberculosis* strain H37Rv mc²6230 (auxotroph) (Fig. 3A to G) and wild-type virulent *M. tuberculosis* strains (Fig. 3H to J) from the Euro-American lineage (H37Rv [Fig. 3H] and Erdman [Fig. 3I]) and a
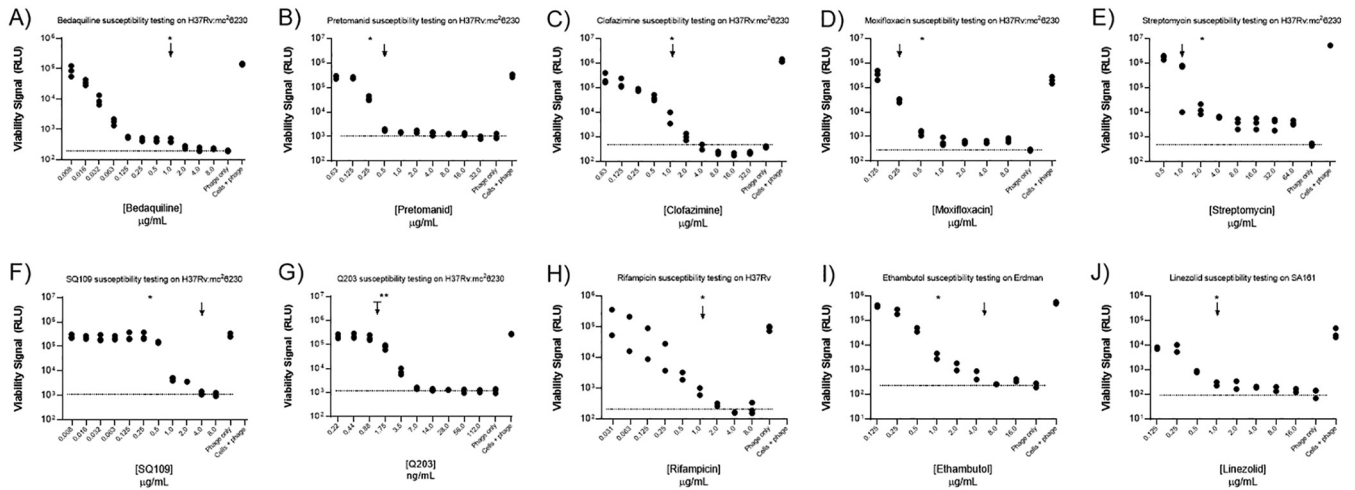
FIG 3 Seventy-two-hour drug susceptibility testing of auxotroph and virulent *M. tuberculosis* strains with a panel of diverse antibiotics. Following a preculture period in rich medium without antibiotic, *M. tuberculosis* cells were washed and resuspended in detergent-free rich medium with a 2-fold dilution series of antibiotic concentrations. After 48 hours of antibiotic exposure, phage was added to wells for a 24-hour infection/nanoluciferase production period. Results are displayed with viability signal (RLU) on the *y* axis and the antibiotic concentration assayed (in ascending order) on the *x* axis. For both the *M. tuberculosis* auxotroph H37Rv mc²6230 (A to G) and virulent clinical *M. tuberculosis* strains H37Rv (H), Erdman (I), and SA161 (J), there is ≥99% inhibition of nanoluciferase light production compared to control wells without antibiotics (indicated by asterisks) within 1 dilution of the antibiotic critical concentration (indicated by arrows). The exceptions to this are for ethambutol treatment of the Erdman strain, which resulted in ≥99% inhibition two dilutions below the critical concentration and, for novel compounds SQ109 and Q203, treatment of H37Rv mc²6230. We observed 99% inhibition of light production following SQ109 treatment only at concentrations 10 times the reported MIC. In the instance of Q203, we benchmarked against the MIC$_{50}$ (capped arrow) and confirmed this value (double asterisks). Dashed lines indicate the noise floor as determined by phage-only background RLU. Antibiotics tested include bedaquiline (A), pretomanid (B), clofazimine (C), moxifloxacin (D), streptomycin (E), SQ109 (F), Q203 (G), rifampin (H), ethambutol (I), and linezolid (J). In all cases, cells plus phage represents the RLU values from infected cells in the absence of antibiotic exposure.

representative of the East Asian-Beijing lineage (SA161 [Fig. 3J]). In these experiments, we prepared 2-fold serial dilution series of antibiotics to flank the WHO-reported critical concentration for each respective drug or the reported MICs for test compounds SQ109 and Q203 (Fig. 3, arrows) (16, 41, 42). After preculture, cells were exposed to antibiotic for 48 hours followed by the addition of TM4-nluc phage and overnight incubation. Accordingly, using this method, cells were exposed to fixed antibiotic concentrations for 48 hours, followed by a 5% reduction of drug exposure concentration for 24 hours (resulting from phage addition [see Materials and Methods]).

For both the H37Rv mc²6230 auxotroph (Fig. 3A to G) and virulent *M. tuberculosis* strains (Fig. 3H to J), we observed inhibition of Nluc production in a dose-response correlated with antibiotic exposure. As a measure of viability and antibiotic susceptibility, RLU production decreased as antibiotic concentration increased, and we observed ≥99% inhibition of RLU signal below or within one dilution of the critical concentration for each antibiotic tested (Fig. 3, asterisks). The lone exception to this pattern was observed with H37Rv mc²6230 exposed to SQ109, for which 99% inhibition of RLU signal was observed at ~10 times the reported MIC (43). At the lowest drug treatment levels, the measured RLU approximated those of the cells plus phage wells (without antibiotics), whereas at supra-MIC antibiotic concentrations, the luminescence approximated that of the phage-only negative-control wells. These data suggest that using this system as a measure of antibiotic susceptibility can be achieved for antibiotics exerting diverse mechanisms of action. In keeping with the concept that phage-mediated viability tests are proxies for metabolic homeostasis, we anticipated that reduction of ATP content through treatment with the ATP synthase inhibitor, bedaquiline (Fig. 3A), or electron transport chain targeting, Q203 (Fig. 3G), would have profound consequences for the production of the TM4-delivered DNA construct. Similarly, the performance of this system as a readout for the activity of antibiotics that inhibit core processes of DNA transcription (rifampin [Fig. 3H]) and RNA translation (streptomycin [Fig. 3E] and linezolid [Fig. 3J]) is anticipated. Under the experimental conditions used here, pretomanid (Fig. 3B) and ethambutol (Fig. 3I) are cell wall-active antibiotics
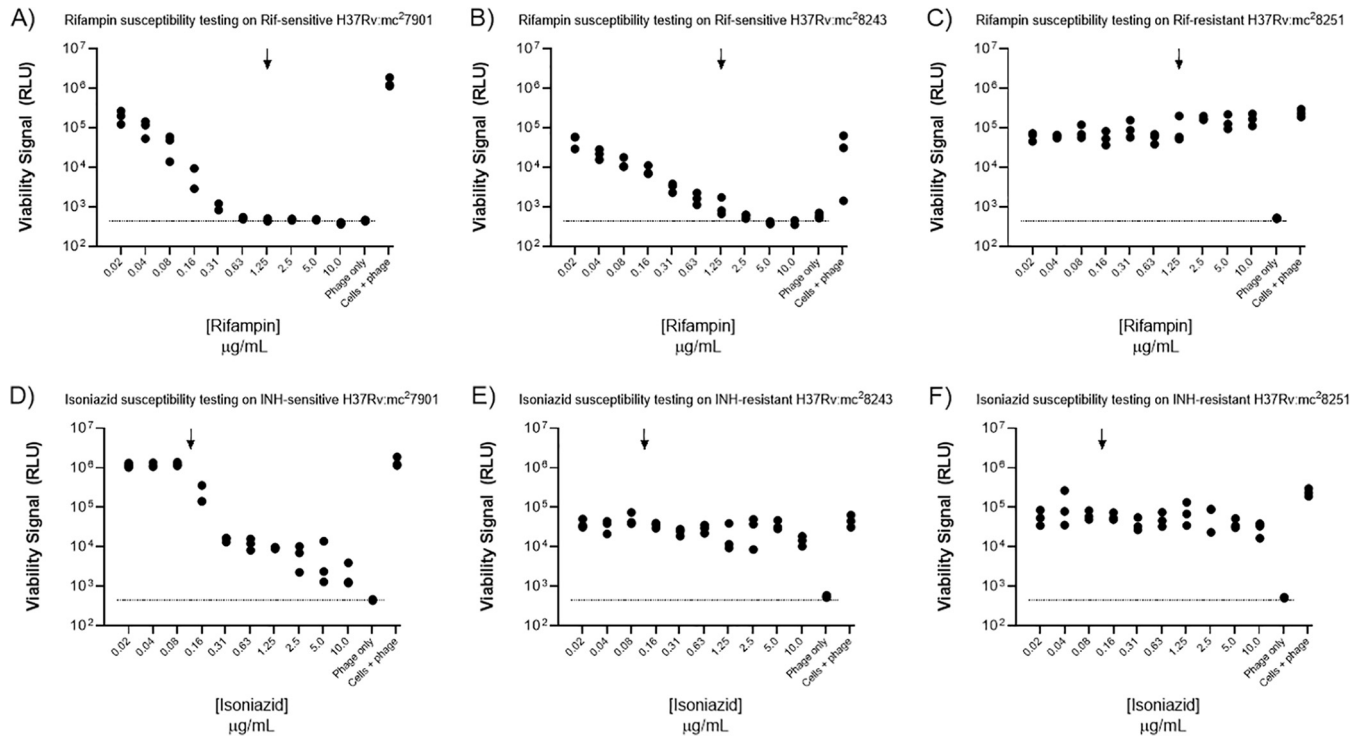
FIG 4 Using defined drug-sensitive and -resistant *M. tuberculosis* auxotrophs TM4-nluc enables 72-hour resistance testing of rifampin and isoniazid. Following a preculture period in rich medium without antibiotic, *M. tuberculosis* cells were washed and resuspended in detergent-free rich medium with a 10-step, 2-fold dilution series of antibiotics, rifampin (A to C) or isoniazid (D to F). The pan-susceptible isogenic parent strain, H37Rv mc²7901 (A to C), demonstrates a dose-dependent inhibition of nanoluciferase light production for both rifampin and isoniazid at or below the critical concentration (indicated by an arrow). The rifampin-sensitive/isoniazid monoresistant strain H37Rv mc²8243 (*katG* W728stop) demonstrates a dose-dependent inhibition of nanoluciferase light production upon exposure to rifampin (B) but light production approximating the untreated control in the isoniazid series (E). In the isoniazid- and rifampin-resistant MDR strain H37Rv mc²8251 (*katG* S315N *rpoB* H445Y), there is no reduction in nanoluciferase signal generated regardless of the antibiotic, or treatment concentration, up to 10 times the critical concentration for rifampin (C) and 100 times the critical concentration for isoniazid (F). Results are displayed with viability signal (RLU) on the *y* axis and the antibiotic concentration assayed (in ascending order) on the *x* axis. Dashed lines indicate the noise floor as determined by phage-only background RLU. In all cases, cells plus phage represents the RLU values from infected cells in the absence of antibiotic exposure.

rather than inhibitors of "central dogma" functions, and the decreased production of the Nluc reporter suggests at least a 2-step readout of sensitivity beginning with disruption of structural physiology of the cell and subsequent perturbation to transcription-translation machinery. The mechanism-agnostic nature of the phage-mediated approach is demonstrated further from the results interrogating the impact of antibiotics that inhibit DNA replication (moxifloxacin [Fig. 3D]) and antibiotics with uncertain (clofazimine [Fig. 3C]) or multiple (SQ109 [Fig. 3F]) mechanisms of action.

Drug susceptibility testing with drug-resistant *M. tuberculosis* auxotrophs: isoniazid and MDR. Results reported above assess TM4-nluc performance in the cellular limit of detection and in the context of susceptibility testing for a range of antibiotics against drug-susceptible auxotrophic and virulent clinical *M. tuberculosis* strains. To understand performance of the TM4-nluc system in drug resistance testing, we used two different drug-resistant *M. tuberculosis* auxotrophic strains: an isoniazid-monoresistant strain (H37Rv mc²8243; *katG* W728stop) and an isoniazid- and rifampin-resistant MDR strain (H37Rv mc²8251; *katG* S315N, *rpoB* H445Y) (35).

For both rifampin (Fig. 4A to C) and isoniazid (Fig. 4D to F), there is a dose-dependent inhibition of Nluc production and luminescent signal generation in the drug-sensitive isogenic control strain (H37Rv mc²7901). For rifampin treatment of the rifampin-resistant auxotroph H37Rv mc²8251, we were unable to detect any decrease in light production, with drug concentrations in excess of 10-fold the rifampin MIC. Similarly, for two genotypically distinct isoniazid-resistant strains, isoniazid exposure failed to result in a decrease in Nluc/luminescence production. In aggregate, these results indicate that the TM4-nluc reagent and experimental system described here are

capable of identifying drug susceptibility and drug resistance for two frontline antibiotics, rifampin and isoniazid. In addition, these results support the use of TM4-nluc in identifying antibiotic monoresistance, as well as combinatorial resistance, accurately identifying an *M. tuberculosis* auxotroph strain with a defined MDR genotype/phenotype compared to the isogenic drug-sensitive parent strain.

DISCUSSION

This work describes the development of an improved reporter mycobacteriophage, TM4-nluc, and its validation for detection and phenotypic DST of *M. tuberculosis*. This reporter phage demonstrates high sensitivity and a cellular limit of detection of $\leq 10^2$ *M. tuberculosis* CFU. By interrogating TM4-nluc performance in DST assays with multiple drug-sensitive and -resistant strains of *M. tuberculosis* (auxotroph and virulent), we demonstrate that a preculture followed by a standardized 72-hour drug exposure-to-result period generates accurate DST results for multiple first- and second-line antitubercular antibiotics with varied mechanisms of action, including all components of the BPaL regimen.

In this work, all experiments were conducted with *M. tuberculosis* isolates in an *in vitro* preculture and culture environment. We observed that a critical parameter to achieve maximum cellular sensitivity is metabolic homeostasis. This was demonstrated in experiments determining the LOD, with brighter signal and improved assay sensitivity when comparing results from 72-hour experiments versus 24 hours (Fig. 2). In both cases, the total infection time was the same; however, the 72-hour experiment included an adaptation period of 48 hours, whereas the shorter duration experiment was designed with phage infection proceeding immediately after cells were placed in fresh (detergent-free) growth medium. While there may be alternate explanations, we considered likely causes to be (i) increased incubation time allowing for additional replications in the 72-hour condition with a commensurate increase in signal due to increased cell number, (ii) increased acclimation time in detergent-free medium allowing for a longer recovery/*M. tuberculosis* cell wall restructuring to a more phage-permissive state, or (iii) increased acclimation time in detergent-free medium allowing for metabolic recovery under altered growth conditions and therefore resulting in more robust expression of the introduced reporter cassette. Despite an additional 48 hours in the plate at 37°C, the cell numbers per well were not dramatically different between the 24- and 72-hour conditions, corresponding to less than 1 cell division. From our data, we cannot definitively distinguish between cell wall restructuring and metabolic recovery; however, if we consider these to be variations on the theme of homeostasis, then our results reinforce importance of cell health as a critical determinant underlying phage-mediated viability monitoring.

Expanding on "metabolic homeostasis" within a population of genotypically identical organisms, the concept of *M. tuberculosis* phenotypic heterogeneity has received substantial attention through studies monitoring responses of single cells or microcolonies (44–47), and previous work with isoniazid susceptibility testing using the green fluorescent protein (GFP) fluorophage ϕ^2GFP10 has demonstrated that mycobacteriophages are capable of distinguishing variable phenotypic drug susceptibilities of individual cells within a genotypically uniform larger population (31). In the case of the TM4-nluc described here, the reporter signal output is a reflection of the entire population of cells assayed, rather than the phenotypic state of a single cell. We observed that the luminescence signal from cells treated with the highest concentrations of drug was elevated compared to the phage-only background (streptomycin [Fig. 3E]; isoniazid [Fig. 4D]), and we speculate that these signals were possibly derived from a minority population that maintained metabolic activity in spite of exposure to high concentrations of antibiotics (31, 48). Accordingly, testing an antibiotic phenotypic response in a stable rich environment enables differentiation of strains with subtly different susceptibility responses. This raises the possibility of using phages bearing different reporter cassettes to explore different aspects of *M. tuberculosis* response to perturbation, ranging from basic/foundational research with single-cell monitoring

using fluorophages to deriving rapid viability data from populations of cells with luminescent phages like TM4-nluc, described here.

Considering drug susceptibility testing, particularly for antibiotics with diverse, or ill-defined, mechanisms of action and resistance mutations, the results reported here extend on previous work that has demonstrated the ability of TM4 to provide readouts on cellular responses to antibiotic exposure (25–34, 49). With TM4-nluc, we observed that there is an antibiotic dose-dependent inhibition of luciferase signal for all test antibiotics interrogated here (rifampin, isoniazid, ethambutol, moxifloxacin, clofazimine, bedaquiline, pretomanid, linezolid, SQ109, and Q203) (Fig. 3 and 4). While this is not a comprehensive list of antitubercular antibiotics, the diversity of mechanisms of action that are compatible with phage-mediated viability monitoring suggest that this approach could be valuable in the context of research and development for novel compound screening or as a comparatively rapid phenotypic DST reference complement to genotypic methods. In support of this, for all compounds tested on antibiotic-susceptible strains, we observed a dose-response inhibition of Nluc production after TM4-nluc infection. With the exception of SQ109, for all compounds, there was a ≥99% inhibition of signal below or within one drug dilution of the MIC, including all components of the BPaL regimen (Fig. 3). Testing SQ109, we observed a concentration-dependent dose-response pattern to Nluc RLU production; however, drug concentrations of approximately 10 times the reported MIC were required to achieve 99% inhibition. We hypothesize that there is a slow perturbation of *M. tuberculosis* metabolism when exposed to SQ109, and this may represent a case in which additional assay optimization is required to align growth- versus phage-based MIC values. The observation that there is a dose-response curve in the phage assay suggests that correlations between clinical cutoffs and *in vitro* assays can be identified. As a critical extension to drug susceptibility testing, we used TM4-nluc for identification of strains with drug resistance to both rifampin (monoresistant) (Fig. 4A to C) or rifampin and isoniazid/MDR resistance (Fig. 4D to F). We did not assess other combinations of drug resistance genotypes/phenotypes, but our combined results lead us to hypothesize that TM4-nluc can be used to identify *M. tuberculosis* strains with combinatorial susceptibility/resistance profiles, ranging across antibiotic classes and resistance phenotypes.

These data support the use of TM4-nluc in the context of interrogating *M. tuberculosis* viability/metabolic homeostasis in response to different antibiotic treatments or compound screens and potentially as a tool for characterizing genotype-phenotype relationships of wild-type and mutant *M. tuberculosis* strains in response to different environments or chemical treatments. Here, all experiments were conducted on cultured *M. tuberculosis*; however, previous studies with ffLuc or green fluorescent protein (ϕ^2GFP10) reporter phages demonstrated that TM4-based reporter phages are compatible with clinical/sputum-derived samples after disinfection with sodium hydroxide (NaOH) (29, 31, 32). Those reports found that NaOH treatment removes mycobacteriophage receptors, thus necessitating culturing of *M. tuberculosis* prior to phage analysis. The enhanced activity of the TM4-nluc system (brighter signal, improved cellular limit of detection) should shorten the time to detection over previous studies on clinical samples. This, in combination with the incorporation of *p*-nitro-α-acetylamino-β-hydroxy propiophenone to distinguish between *M. tuberculosis* and nontuberculous mycobacteria (26), should allow for the application of this system on clinical samples. With additional validation on expanded libraries of both drug-sensitive and -resistant clinical strains of *M. tuberculosis*, we anticipate the value of phage-mediated quantitative DST as a complement to molecular/genotypic DST in clinical reference settings. In this regard, the potential diagnostic capacity of most phenotypic and molecular DST methods is underutilized, as they are used in a binary, or one-size-fits-all, approach. In the absence of routine quantitative DST, *M. tuberculosis* strains are simply identified only as susceptible or resistant without determination of the level of drug resistance, the presence and level of antibiotic cross-resistance, and the impact of associated achievable drug concentration. This may lead to unnecessary discontinuation of a key drug or incorrect diagnosis of an individual as an MDR-TB or XDR-TB patient. Therefore,

TABLE 1 Strains used in this study

Strain	Species	Genotype	Drug resistance[a]	Reference no.
mc^{2}6230	*M. tuberculosis*	Δ*panCD* Δ*RD1*		31, 61
mc^{2}6206	*M. tuberculosis*	Δ*leuCD* Δ*panCD*		57
mc^{2}7901	*M. tuberculosis*	Δ*leuCD* Δ*panCD* Δ*metA*		35
mc^{2}8243	*M. tuberculosis*	Δ*leuCD* Δ*panCD* Δ*metA katG* W728stop	INH	35
mc^{2}8251	*M. tuberculosis*	Δ*leuCD* Δ*panCD* Δ*metA rpoB* H445Y *katG* S315N	INH, RIF	35
mc^{2}155	*M. smegmatis*	EptB1 stop(Ochre)241L EptC1 K3stop(Ochre)		58, 62

[a]INH, isoniazid; RIF, rifampin.

sensitive quantitative phenotypic DST approaches such as the system described here can play a critical role in validating the clinical significance of a specific mutation in a particular patient or in identifying new mutations with unknown phenotypic and clinical impact. The genotype-agnostic nature of the readout, the breadth of compatible antibiotics/mechanisms of action demonstrated already, and the potential to interrogate phenotypic responses under a range of environmental conditions all suggest value in more widespread use of TM4-nluc.

MATERIALS AND METHODS

Culturing methods. All the mycobacterial strains used in this study were obtained from laboratory stocks and are listed in Table 1. Mycobacterial cells were resuscitated from glycerol stock in fully supplemented 7H9 media to an optical density at 600 nm (OD$_{600}$) of 1.0 and used as a seed culture to subculture for the next 3 weeks before going back to the glycerol stocks. Routinely, 10 ml of mycobacterial cultures was grown in 50-ml conical vials by incubating on a Cel-Gro tissue culture rotator wheel (Thermo Scientific) at 37°C. Middlebrook 7H9 supplemented with 0.5% glycerol (vol/vol), 0.10% Tween 80, and 10% albumin-dextrose-catalase (ADC; BD Biosciences) was used a liquid culture medium. 7H10 agar supplemented with 10% oleic acid-albumin-dextrose-catalase (OADC; BD Biosciences), 0.5% glycerol (vol/vol), and 0.10% Tween 80 was used as a solid culture medium. Wherever needed, nutrient supplements were used at the following concentrations: 24 μg/ml of calcium pantothenate, 50 μg/ml of methionine, and 50 μg/ml leucine. All the chemicals, unless specified, were obtained from Sigma-Aldrich or Thermo (Fisher) Scientific.

Generation of TM4-nluc phage. *M. tuberculosis* codon-optimized nanoluciferase (nluc$_{M.\ tuberculosis}$) was synthesized by GenScript Biotechnology and cloned into pMV261-derived plasmid (50, 51) using EcoRV/PsiI restriction sites. The resulting plasmid, pYUB2659, expresses Nluc from the pL promoter of bacteriophage L5 (52) and has the following features: a unique PacI site (53), pAL5000 origin of replication (54), 600-bp region flanking D29 cohesive ends (cos site) (55), and lambda cos site (56). The plasmid pYUB2659 was introduced into the TM4-derived phage backbone phAE159 using the standard *in vitro* packaging protocol (57) and electroporated into *M. smegmatis* mc^{2}155 (57, 58) to obtain TM4-nluc phage plaques (Fig. 1). Individual plaques were picked and propagated at 30°C to obtain high-titer TM4-nluc phage (57). Phage titers were determined by spotting 5 μl of 10-fold serial dilution on *M. smegmatis* mc^{2}155 lawns (57). Nluc activity was determined in high-titer phage lysates using the recommended standard procedure (described in "Nanoluciferase activity assay" below).

Removal/separation of background nanoluciferase protein from phage lysates. Two methods were optimized for reduction of Nluc protein present as a by-product in the preparation of TM4-nluc phage lysates: (i) anion-exchange chromatography (AEX) followed by hydrophobic interaction chromatography (HIC) and (ii) ultracentrifugation. Chromatography was performed at ambient temperature, and all centrifugation was performed at 4°C.

(i) AEX. TM4-nluc phage (>10^9 PFU/ml) was mixed 1:1 with AEX-A loading buffer (to a final concentration of 10 mM MgCl$_2$, 2 mM CaCl$_2$, 50 mM Tris-Cl [pH 6.7], and 0.05% Tween 80) and loaded, at 3 ml/min, on a disposable NatriFlo HD-Q membrane adsorber (Millipore) column preequilibrated with AEX-A buffer. The column was washed with a 10-bed volume of AEX-A buffer followed by a 100-bed-volume wash with AEX-A buffer containing 250 mM NaCl (AEX-B). Bound phages were eluted by a step gradient at 1 M NaCl in AEX-A buffer (AEX-C) and collected in 1-ml fractions. Purified fractions with the highest phage titer/Nluc (titer and Nluc activity determined as described) activity ratio were pooled and used for HIC.

(ii) HIC. Ammonium sulfate concentration was increased to 700 mM in the pooled fraction by dropwise addition of (NH$_4$)$_2$SO$_4$-saturated AEX-A buffer with constant stirring (59). The sample was loaded on a HiTrap butyl FF column at 1 ml/min and on a column preequilibrated with HIC-A [AEX-A with 700 mM (NH$_4$)$_2$SO$_4$], followed by a wash with a 10-bed volume of the same. Bound phages were eluted by a 36-bed-volume linear gradient of 700-0 mM (NH$_4$)$_2$SO$_4$ in AEX-A buffer followed by a final 12-bed-volume elution with AEX-A. One-milliliter fractions were collected and pooled into two groups, based on phage titer/Nluc activity ratio.

(iii) Buffer exchange. Pooled fractions were centrifuged at 20,000 × *g* for 3 hours at 6°C in high-*g* polypropylene centrifuge tubes. The supernatant was gently removed, and the phage pellet was resuspended in mycobacteriophage (MP) buffer overnight without shaking at 4°C. Phage titer/Nluc activity was determined prior to subsequent use.

(iv) TM4-nluc purification by ultracentrifugation. Briefly, cesium chloride (CsCl) solution (density, 1.54 g/ml) was prepared by dissolving 100 g of molecular biology-grade cesium chloride (Merck Millipore, USA; catalog no. 219650) in 100 ml of water and filtered through a 0.22-μM membrane filter. We transferred 25 ml of this solution to 38.5-ml ultraclear tubes (Beckman Coulter, USA; catalog no. 344058), and 13 ml of TM4-nluc lysate in MP buffer (prepared as described above) was layered slowly above the CsCl solution. Tubes were centrifuged for 22 h at 28,000 rpm (96,281 $\times$ g) at 4°C in a swinging-bucket rotor (SW 32 Ti) (Beckman Coulter, USA). Following centrifugation, tubes contained three visible fractions, which were individually collected starting from the top layer by means of puncturing with an 18-gauge needle. RLU and titers of fractions were measured as described above. The top and bottom layer fractions were low yield and discarded. The middle layer fraction had the optimal RLU/titer ratio and was used in further assays.

LOD and phenotypic DST assays. From glycerol stock, *M. tuberculosis* cells were inoculated to a target OD_{600} of ~0.1 in 10 ml fully supplemented 7H9 medium containing Tween 80. Cells were incubated for 72 hours at 37°C with agitation. Following this preculture period, the resultant *M. tuberculosis* cells were washed twice with detergent-free (fully supplemented 7H9 without Tween 80) medium and resuspended in the same medium to a final OD_{600} of 0.1 to 0.2. Cells were incubated as standing culture for 24 hours at 37°C prior to LOD and DST assay setup.

(i) LOD. We aliquoted 90 μl of 10-fold serially diluted cells in four sets of triplicates in 96-well flat-bottom plates. Two sets were used for each 24- and 72-hour LOD determination. For the 24-hour LOD, 10 μl of phage was immediately added to one set, and the other set of 10-fold serially diluted cells was plated for CFU enumeration on 7H10 agar plates. For the 72-hour LOD, the plates were incubated for an additional 48 hours at 37°C. Subsequently, 10 μl of phage was added to one set, and the other set was plated on 7H10 agar plates for CFU enumeration. The final concentration of phage in each well was 3.5×10^7 PFU/ml. In each case, the plates were incubated at 37°C for 24 additional hours after phage addition, and the nanoluciferase activity was determined using the manufacturer-recommended standard procedure (described in "Nanoluciferase activity assay" below). The number of *M. tuberculosis* cells in each well at the time of phage infection was enumerated by counting for colonies after 3 weeks of incubation at 37°C in a sealed plastic bag.

(ii) DST. Ninety microliters of 2-fold serially diluted drug dilutions was aliquoted in a set of triplicates along with no-drug control triplicate wells. We added 5 μl of *M. tuberculosis* cells with an OD_{600} of 0.1 to 0.2 to 90 μl of drug dilutions and the control wells. The plates were incubated at 37°C for 48 hours before adding 5 μl of phage to each treatment and phage-only control well. The final concentration of phage in each well was 2×10^7 PFU/ml. Plates were incubated at 37°C for 24 additional hours after phage addition, and the nanoluciferase activity was determined using the recommended standard procedure (described in "Nanoluciferase activity assay" below).

Nanoluciferase activity assay. Nanoluciferase activity was determined as recommended in the Nano-Glo luciferase assay system manual. Briefly, Nano-Glo substrate was diluted 1:50 in Nano-Glo buffer and mixed 1:1 (vol/vol) with samples and read on a BioTek Synergy H1 plate reader using the following settings: luminescent fiber, 135 gain, 0.1 s read time, and 1 mm read height. The method and settings were consistent for determination of RLU in *M. smegmatis*/phage propagation, assessment of phage cleanup during purification, and in experiments with auxotroph and virulent *M. tuberculosis*, with the exception that for *M. tuberculosis* experiments, after addition of substrate, plates were covered with adhesive, optically clear plate sealer (Microseal B PCR plate-sealing film, adhesive, optical no. MSB1001; Bio-Rad) and decontaminated, and luminescence was read immediately.

SUPPLEMENTAL MATERIAL

Supplemental material is available online only.
SUPPLEMENTAL FILE 1, PDF file, 0.4 MB.

ACKNOWLEDGMENT

REFERENCES

1. World Health Organization. 2019. Global tuberculosis report 2019. World Health Organization, Geneva, Switzerland.
2. Gandhi NR, Moll A, Sturm AW, Pawinski R, Govender T, Lalloo U, Zeller K, Andrews J, Friedland G. 2006. Extensively drug-resistant tuberculosis as a cause of death in patients co-infected with tuberculosis and HIV in a rural area of South Africa. Lancet 368:1575–1580. https://doi.org/10.1016/S0140-6736(06)69573-1.
3. Raviglione M. 2013. Global strategy and targets for tuberculosis prevention, care and control after 2015. EB134/12. World Health Organization, Geneva, Switzerland.
4. Edwards MC, Gibbs RA. 1994. Multiplex PCR: advantages, development, and applications. PCR Methods Appl 3:S65–75. https://doi.org/10.1101/gr.3.4.s65.
5. Molenkamp R, van der Ham A, Schinkel J, Beld M. 2007. Simultaneous detection of five different DNA targets by real-time Taqman PCR using the Roche LightCycler480: application in viral molecular diagnostics. J Virol Methods 141:205–211. https://doi.org/10.1016/j.jviromet.2006.12.007.
6. Fu G, Miles A, Alphey L. 2012. Multiplex detection and SNP genotyping in a single fluorescence channel. PLoS One 7:e30340. https://doi.org/10.1371/journal.pone.0030340.
7. Walker TM, Kohl TA, Omar SV, Hedge J, Del Ojo Elias C, Bradley P, Iqbal Z, Feuerriegel S, Niehaus KE, Wilson DJ, Clifton DA, Kapatai G, Ip CLC, Bowden R, Drobniewski FA, Allix-Béguec C, Gaudin C, Parkhill J, Diel R, Supply P, Crook DW, Smith EG, Walker AS, Ismail N, Niemann S, Peto TEA, Modernizing Medical Microbiology (MMM) Informatics Group. 2015. Whole-genome sequencing for prediction of Mycobacterium tuberculosis drug susceptibility and resistance: a retrospective cohort study. Lancet Infect Dis 15:1193–1202. https://doi.org/10.1016/S1473-3099(15)00062-6.

8. Helb D, Jones M, Story E, Boehme C, Wallace E, Ho K, Kop J, Owens MR, Rodgers R, Banada P, Safi H, Blakemore R, Lan NT, Jones-Lopez EC, Levi M, Burday M, Ayakaka I, Mugerwa RD, McMillan B, Winn-Deen E, Christel L, Dailey P, Perkins MD, Persing DH, Alland D. 2010. Rapid detection of *Mycobacterium tuberculosis* and rifampin resistance by use of on-demand, near-patient technology. J Clin Microbiol 48:229–237. https://doi.org/10.1128/JCM.01463-09.

9. World Health Organization. 2019. Consolidated guidelines on drug-resistant tuberculosis treatment. World Health Organization, Geneva, Switzerland. https://apps.who.int/iris/bitstream/handle/10665/311389/9789241550529-eng.pdf.

10. World Health Organization. 2019. Rapid communication: key changes to the treatment of drug-resistant tuberculosis. World Health Organization, Geneva, Switzerland.

11. Conradie F, Diacon AH, Ngubane N, Howell P, Everitt D, Crook AM, Mendel CM, Egizi E, Moreira J, Timm J, McHugh TD, Wills GH, Bateson A, Hunt R, Van Niekerk C, Li M, Olugbosi M, Spigelman M, Nix-TB Trial Team. 2020. Treatment of highly drug-resistant pulmonary tuberculosis. N Engl J Med 382:893–902. https://doi.org/10.1056/NEJMoa1901814.

12. Kadura S, King N, Nakhoul M, Zhu H, Theron G, Köser CU, Farhat M. 2020. Systematic review of mutations associated with resistance to the new and repurposed Mycobacterium tuberculosis drugs bedaquiline, clofazimine, linezolid, delamanid and pretomanid. J Antimicrob Chemother https://doi.org/10.1093/jac/dkaa136.

13. Clinical and Laboratory Standards Institute. 2011. Susceptibility testing of Mycobacteria, Nocardiae, and other aerobic Actinomycetes; approved standard, 2nd ed; CLSI document M24-A2. Clinical and Laboratory Standards Institute, Wayne, PA.

14. Leber A. 2016. Tests to assess bactericidal activity. *In* Leber AL (ed), Clinical microbiology procedures handbook, 4th ed, vol 2. ASM Press, Washington, DC.

15. Santos NCS, Scodro RBL, Sampiron EG, Ieque AL, Carvalho HC, Santos TDS, Ghiraldi Lopes LD, Campanerut-Sa PAZ, Siqueira VLD, Caleffi-Ferracioli KR, Teixeira JJV, Cardoso RF. 2020. Minimum bactericidal concentration techniques in *Mycobacterium tuberculosis*: a systematic review. Microb Drug Resist 26:752–765. https://doi.org/10.1089/mdr.2019.0191.

16. World Health Organization. 2018. Technical report on critical concentrations for TB drug susceptibility testing of medicines used in the treatment of drug-resistant TB. World Health Organization, Geneva, Switzerland.

17. Bemer P, Palicova F, Rusch-Gerdes S, Drugeon HB, Pfyffer GE. 2002. Multicenter evaluation of fully automated BACTEC Mycobacteria growth indicator tube 960 system for susceptibility testing of Mycobacterium tuberculosis. J Clin Microbiol 40:150–154. https://doi.org/10.1128/jcm.40.1.150-154.2002.

18. Caviedes L, Lee TS, Gilman RH, Sheen P, Spellman E, Lee EH, Berg DE, Montenegro-James S, The Tuberculosis Working Group in Peru. 2000. Rapid, efficient detection and drug susceptibility testing of *Mycobacterium tuberculosis* in sputum by microscopic observation of broth cultures. J Clin Microbiol 38:1203–1208. https://doi.org/10.1128/JCM.38.3.1203-1208.2000.

19. Lee J, Armstrong DT, Ssengooba W, Park JA, Yu Y, Mumbowa F, Namaganda C, Mboowa G, Nakayita G, Armakovitch S, Chien G, Cho SN, Via LE, Barry CE, III, Ellner JJ, Alland D, Dorman SE, Joloba ML. 2014. Sensititre MYCOTB MIC plate for testing Mycobacterium tuberculosis susceptibility to first- and second-line drugs. Antimicrob Agents Chemother 58:11–18. https://doi.org/10.1128/AAC.01209-13.

20. Choi J, Yoo J, Kim KJ, Kim EG, Park KO, Kim H, Kim H, Jung H, Kim T, Choi M, Kim HC, Ryoo S, Jung YG, Kwon S. 2016. Rapid drug susceptibility test of Mycobacterium tuberculosis using microscopic time-lapse imaging in an agarose matrix. Appl Microbiol Biotechnol 100:2355–2365. https://doi.org/10.1007/s00253-015-7210-0.

21. Ghodbane R, Raoult D, Drancourt M. 2014. Dramatic reduction of culture time of Mycobacterium tuberculosis. Sci Rep 4:4236. https://doi.org/10.1038/srep04236.

22. Palomino JC, Martin A, Camacho M, Guerra H, Swings J, Portaels F. 2002. Resazurin microtiter assay plate: simple and inexpensive method for detection of drug resistance in Mycobacterium tuberculosis. Antimicrob Agents Chemother 46:2720–2722. https://doi.org/10.1128/aac.46.8.2720-2722.2002.

23. Jain P, Thaler DS, Maiga M, Timmins GS, Bishai WR, Hatfull GF, Larsen MH, Jacobs WR. 2011. Reporter phage and breath tests: emerging phenotypic assays for diagnosing active tuberculosis, antibiotic resistance, and

treatment efficacy. J Infect Dis 204(Suppl 4):S1142–50. https://doi.org/10.1093/infdis/jir454.

24. Meile S, Kilcher S, Loessner MJ, Dunne M. 2020. Reporter phage-based detection of bacterial pathogens: design guidelines and recent developments. Viruses 12:E944. https://doi.org/10.3390/v12090944.

25. Jacobs WR, Jr., Barletta RG, Udani R, Chan J, Kalkut G, Sosne G, Kieser T, Sarkis GJ, Hatfull GF, Bloom BR. 1993. Rapid assessment of drug susceptibilities of Mycobacterium tuberculosis by means of luciferase reporter phages. Science 260:819–822. https://doi.org/10.1126/science.8484123.

26. Riska PF, Jacobs WR, Bloom BR, McKitrick J, Chan J. 1997. Specific identification of Mycobacterium tuberculosis with the luciferase reporter mycobacteriophage: use of p-nitro-alpha-acetylamino-beta-hydroxy propiophenone. J Clin Microbiol 35:3225–3231. https://doi.org/10.1128/JCM.35.12.3225-3231.1997.

27. Carriere C, Riska PF, Zimhony O, Kriakov J, Bardarov S, Burns J, Chan J, Jacobs WR, Jr. 1997. Conditionally replicating luciferase reporter phages: improved sensitivity for rapid detection and assessment of drug susceptibility of Mycobacterium tuberculosis. J Clin Microbiol 35:3232–3239. https://doi.org/10.1128/JCM.35.12.3232-3239.1997.

28. Bardarov S, Jr., Dou H, Eisenach K, Banaiee N, Ya S, Chan J, Jacobs WR, Jr., Riska P. 2003. Detection and drug-susceptibility testing of M. tuberculosis from sputum samples using luciferase reporter phage: comparison with the Mycobacteria Growth Indicator Tube (MGIT) system. Diagn Microbiol Infect Dis 45:53–61. https://doi.org/10.1016/S0732-8893(02)00478-9.

29. Banaiee N, Bobadilla-Del-Valle M, Bardarov S, Riska P, Small P, Ponce-De-Leon A, Jacobs W, Hatfull G, Sifuentes-Osornio J. 2001. Luciferase reporter mycobacteriophages for detection, identification, and antibiotic susceptibility testing of Mycobacterium tuberculosis in Mexico. J Clin Microbiol 39:3883–3888. https://doi.org/10.1128/JCM.39.11.3883-3888.2001.

30. Banaiee N, Bobadilla-del-Valle M, Riska PF, Bardarov S, Jr., Small PM, Ponce-de-Leon A, Jacobs WR, Jr., Hatfull GF, Sifuentes-Osornio J. 2003. Rapid identification and susceptibility testing of Mycobacterium tuberculosis from MGIT cultures with luciferase reporter mycobacteriophages. J Med Microbiol 52:557–561. https://doi.org/10.1099/jmm.0.05149-0.

31. Jain P, Hartman TE, Eisenberg N, O'Donnell MR, Kriakov J, Govender K, Makume M, Thaler DS, Hatfull GF, Sturm AW, Larsen MH, Moodley P, Jacobs WR, Jr. 2012. phi(2)GFP10, a high-intensity fluorophage, enables detection and rapid drug susceptibility testing of *Mycobacterium tuberculosis* directly from sputum samples. J Clin Microbiol 50:1362–1369. https://doi.org/10.1128/JCM.06192-11.

32. O'Donnell MR, Larsen MH, Brown TS, Jain P, Munsamy V, Wolf A, Uccellini L, Karim F, de Oliveira T, Mathema B, Jacobs WR, Pym A. 2019. Early detection of emergent extensively drug-resistant tuberculosis by flow cytometry-based phenotyping and whole-genome sequencing. Antimicrob Agents Chemother 63:e01834-18. https://doi.org/10.1128/AAC.01834-18.

33. Rondon L, Urdaniz E, Latini C, Payaslian F, Matteo M, Sosa EJ, Do Porto DF, Turjanski AG, Nemirovsky S, Hatfull GF, Poggi S, Piuri M. 2018. Fluoromycobacteriophages can detect viable *Mycobacterium tuberculosis* and determine phenotypic rifampicin resistance in 3–5 days from sputum collection. Front Microbiol 9:1471. https://doi.org/10.3389/fmicb.2018.01471.

34. Jain P, Weinrick BC, Kalivoda EJ, Yang H, Munsamy V, Vilcheze C, Weisbrod TR, Larsen MH, O'Donnell MR, Pym A, Jacobs WR, Jr. 2016. Dual-reporter mycobacteriophages (Phi2DRMs) reveal preexisting Mycobacterium tuberculosis persistent cells in human sputum. mBio 7:e01023-16. https://doi.org/10.1128/mBio.01023-16.

35. Vilcheze C, Copeland J, Keiser TL, Weisbrod T, Washington J, Jain P, Malek A, Weinrick B, Jacobs WR. Jr., 2018. Rational design of biosafety level 2-approved, multidrug-resistant strains of Mycobacterium tuberculosis through nutrient auxotrophy. mBio 9:e00938-18. https://doi.org/10.1128/mBio.00938-18.

36. Hall MP, Unch J, Binkowski BF, Valley MP, Butler BL, Wood MG, Otto P, Zimmerman K, Vidugiris G, Machleidt T, Robers MB, Benink HA, Eggers CT, Slater MR, Meisenheimer PL, Klaubert DH, Fan F, Encell LP, Wood KV. 2012. Engineered luciferase reporter from a deep sea shrimp utilizing a novel imidazopyrazinone substrate. ACS Chem Biol 7:1848–1857. https://doi.org/10.1021/cb3002478.

37. England CG, Ehlerding EB, Cai W. 2016. NanoLuc: a small luciferase is brightening up the field of bioluminescence. Bioconjug Chem 27:1175–1187. https://doi.org/10.1021/acs.bioconjchem.6b00112.

38. Nesbit CE, Levin ME, Donnelly-Wu MK, Hatfull GF. 1995. Transcrip-

tional regulation of repressor synthesis in mycobacteriophage L5. Mol Microbiol 17:1045–1056. https://doi.org/10.1111/j.1365-2958.1995.mmi_17061045.x.

39. Holstein CA, Griffin M, Hong J, Sampson PD. 2015. Statistical method for determining and comparing limits of detection of bioassays. Anal Chem 87:9795–9801. https://doi.org/10.1021/acs.analchem.5b02082.

40. Ritz C, Baty F, Streibig JC, Gerhard D. 2015. Dose-response analysis using R. PLoS One 10:e0146021. https://doi.org/10.1371/journal.pone.0146021.

41. Lee RE, Protopopova M, Crooks E, Slayden RA, Terrot M, Barry C. 2003. Combinatorial lead optimization of [1, 2]-diamines based on ethambutol as potential antituberculosis preclinical candidates. J Comb Chem 5:172–187. https://doi.org/10.1021/cc020071p.

42. Pethe K, Bifani P, Jang J, Kang S, Park S, Ahn S, Jiricek J, Jung J, Jeon HK, Cechetto J, Christophe T, Lee H, Kempf M, Jackson M, Lenaerts AJ, Pham H, Jones V, Seo MJ, Kim YM, Seo M, Seo JJ, Park D, Ko Y, Choi I, Kim R, Kim SY, Lim SBin, Yim S-A, Nam J, Kang H, Kwon H, Oh C-T, Cho Y, Jang Y, Kim J, Chua A, Tan BH, Nanjundappa MB, Rao SPS, Barnes WS, Wintjens R, Walker JR, Alonso S, Lee S, Kim J, Oh S, Oh T, Nehrbass U, Han S-J, No Z, et al. 2013. Discovery of Q203, a potent clinical candidate for the treatment of tuberculosis. Nat Med 19:1157–1160. https://doi.org/10.1038/nm.3262.

43. Sacksteder KA, Protopopova M, Barry CE, Andries K, Nacy C. 2012. Discovery and development of SQ109: a new antitubercular drug with a novel mechanism of action. Future Microbiol 7:823–837. https://doi.org/10.2217/fmb.12.56.

44. Herricks T, Donczew M, Mast FD, Rustad T, Morrison R, Sterling TR, Sherman DR, Aitchison JDJE. 2020. ODELAM rapid sequence-independent detection of drug resistance in isolates of Mycobacterium tuberculosis. Elife 9:e56613. https://doi.org/10.7554/eLife.56613.

45. Dhar N, McKinney J, Manina G. 2016. Phenotypic heterogeneity in Mycobacterium tuberculosis. Microbiol Spectr 4. https://doi.org/10.1128/microbiolspec.TBTB2-0021-2016.

46. Cadena AM, Fortune SM, Flynn JL. 2017. Heterogeneity in tuberculosis. Nat Rev Immunol 17:691–702. https://doi.org/10.1038/nri.2017.69.

47. Aldridge BB, Keren I, Fortune SM. 2014. The spectrum of drug susceptibility in mycobacteria. Microbiol Spectr 2. https://doi.org/10.1128/microbiolspec.MGM2-0031-2013.

48. Manina G, Dhar N, McKinney J, microbe. 2015. Stress and host immunity amplify Mycobacterium tuberculosis phenotypic heterogeneity and induce nongrowing metabolically active forms. Cell Host Microbe 17:32–46. https://doi.org/10.1016/j.chom.2014.11.016.

49. O'Donnell MR, Pym A, Jain P, Munsamy V, Wolf A, Karim F, Jacobs WR, Jr., Larsen MH. 2015. A novel reporter phage to detect tuberculosis and rifampin resistance in a high-HIV-burden population. J Clin Microbiol 53:2188–2194. https://doi.org/10.1128/JCM.03530-14.

50. Stover CK, de la Cruz VF, Fuerst TR, Burlein JE, Benson LA, Bennett LT, Bansal GP, Young JF, Lee MH, Hatfull GF. 1991. New use of BCG for recombinant vaccines. Nature 351:456–460. https://doi.org/10.1038/351456a0.

51. Jacobs WR, Jr., Tuckman M, Bloom BR. 1987. Introduction of foreign DNA into mycobacteria using a shuttle phasmid. Nature 327:532–535. https://doi.org/10.1038/327532a0.

52. Brown KL, Sarkis GJ, Wadsworth C, Hatfull GF. 1997. Transcriptional silencing by the mycobacteriophage L5 repressor. EMBO J 16:5914–5921. https://doi.org/10.1093/emboj/16.19.5914.

53. Bardarov S, Kriakov J, Carriere C, Yu S, Vaamonde C, McAdam RA, Bloom BR, Hatfull GF, Jacobs WR, Jr. 1997. Conditionally replicating mycobacteriophages: a system for transposon delivery to Mycobacterium tuberculosis. Proc Natl Acad Sci U S A 94:10961–10966. https://doi.org/10.1073/pnas.94.20.10961.

54. Gicquel-Sanzey B, Moniz-Pereira J, Gheorghiu M, Rauzier J. 1989. Structure of pAL5000, a plasmid from M. fortuitum and its utilization in transformation of mycobacteria. Acta Leprol 7(Suppl 1):208–211.

55. Ford ME, Sarkis GJ, Belanger AE, Hendrix RW, Hatfull GF. 1998. Genome structure of mycobacteriophage D29: implications for phage evolution. J Mol Biol 279:143–164. https://doi.org/10.1006/jmbi.1997.1610.

56. Feiss M, Kobayashi I, Widner W. 1983. Separate sites for binding and nicking of bacteriophage lambda DNA by terminase. Proc Natl Acad Sci U S A 80:955–959. https://doi.org/10.1073/pnas.80.4.955.

57. Jain P, Hsu T, Arai M, Biermann K, Thaler DS, Nguyen A, Gonzalez PA, Tufariello JM, Kriakov J, Chen B, Larsen MH, Jacobs WR, Jr. 2014. Specialized transduction designed for precise high-throughput unmarked deletions in Mycobacterium tuberculosis. mBio 5:e01245-14–e01214. https://doi.org/10.1128/mBio.01245-14.

58. Panas MW, Jain P, Yang H, Mitra S, Biswas D, Wattam AR, Letvin NL, Jacobs WR, Jr. 2014. Noncanonical SMC protein in Mycobacterium smegmatis restricts maintenance of Mycobacterium fortuitum plasmids. Proc Natl Acad Sci U S A 111:13264–13271. https://doi.org/10.1073/pnas.1414207111.

59. Wood WI. 1976. Tables for the preparation of ammonium sulfate solutions. Anal Biochem 73:250–257. https://doi.org/10.1016/0003-2697(76)90165-2.

60. Bardarov S, Bardarov S, Pavelka MS, Sambandamurthy V, Larsen M, Tufariello J, Chan J, Hatfull G, Jacobs WR. 2002. Specialized transduction: an efficient method for generating marked and unmarked targeted gene disruptions in Mycobacterium tuberculosis, M. bovis BCG and M. smegmatis. Microbiology (Reading) 148:3007–3017. https://doi.org/10.1099/00221287-148-10-3007.

61. Sambandamurthy VK, Derrick SC, Hsu T, Chen B, Larsen MH, Jalapathy KV, Chen M, Kim J, Porcelli SA, Chan J, Morris SL, Jacobs WR, Jr. 2006. Mycobacterium tuberculosis DeltaRD1 DeltapanCD: a safe and limited replicating mutant strain that protects immunocompetent and immunocompromised mice against experimental tuberculosis. Vaccine 24:6309–6320. https://doi.org/10.1016/j.vaccine.2006.05.097.

62. Snapper SB, Melton RE, Mustafa S, Kieser T, Jacobs WR, Jr. 1990. Isolation and characterization of efficient plasmid transformation mutants of Mycobacterium smegmatis. Mol Microbiol 4:1911–1919. https://doi.org/10.1111/j.1365-2958.1990.tb02040.x.